Published in final edited form as:
Cell Stem Cell. 2010 December 3; 7(6): 682–693. doi:10.1016/j.stem.2010.11.013.

Bmi-1 is a Crucial Regulator of Prostate Stem Cell Self-Renewal and Malignant Transformation

Rita U. Lukacs[1], **Sanaz Memarzadeh**[2], **Hong Wu**[3,4], and **Owen N. Witte**[1,3,4,5]

[1]Department of Microbiology, Immunology and Molecular Genetics, University of California, Los Angeles

[2]Department of Obstetrics and Gynecology, David Geffen School of Medicine, University of California, Los Angeles

[3]Department of Molecular and Medical Pharmacology, David Geffen School of Medicine, University of California, Los Angeles

[4]Eli and Edythe Broad Center of Regenerative Medicine and Stem Cell Research, University of California, Los Angeles,

[5]Howard Hughes Medical Institute, University of California, Los Angeles.

SUMMARY

The Polycomb group transcriptional repressor Bmi-1 is often up-regulated in prostate cancer, but its functional roles in prostate stem cell maintenance and prostate cancer are unclear. Loss- and gain-of-function analysis in a prostate sphere assay indicates that Bmi-1 expression is required for self-renewal activity and maintenance of p63+ stem cells. Loss of Bmi-1 blocks the self-renewal activity induced by heightened beta-catenin signaling, suggesting that Bmi-1 is required for full activity of another self-renewal pathway. *In vivo*, Bmi-1 expression is necessary for normal prostate tubule regeneration. Altered self-renewal and proliferation through Bmi-1 modulation diminishes the susceptibility of prostate cells to transformation. In an *in vivo* prostate regeneration system, Bmi-1 inhibition protects prostate cells from FGF10 driven hyperplasia and slows the growth of aggressive Pten-deletion induced prostate cancer. We conclude that Bmi-1 is a crucial regulator of self-renewal in adult prostate cells, and plays important roles in prostate cancer initiation and progression.

INTRODUCTION

Adult stem cells require self-renewal to maintain organ homeostasis and replenish the stem cell pool after tissue injury (He et al., 2009). Self-renewal mechanisms that allow stem cells to persist usually involve proto-oncogenic pathways such as Wnt, Shh, Notch, and the polycomb group genes (Gil et al., 2005; Reya et al., 2001). Components of these tissue specific self-renewal pathways are found mutated or up-regulated in many malignancies, and have been shown to contribute to cancer progression (Pardal et al., 2005).

Corresponding author: Owen N. Witte, M.D. Howard Hughes Medical Institute University of California, Los Angeles 675 Charles E. Young Dr. South 5-748 MRL Los Angeles, CA 90095-1662 Phone: 310-206-0386 FAX: 310-206-8822 owenwitte@mednet.ucla.edu .

The Polycomb-group transcriptional repressor Bmi-1 has emerged as a key regulator in several cellular processes including stem cell self-renewal and cancer cell proliferation. Bmi-1 was first identified in 1991 as a frequent target of Moloney virus insertion in virally accelerated B-lymphoid tumors of E mu-myc transgenic mice (van Lohuizen et al., 1991). The main target of Bmi-1 repression is the Cdkn2a locus, which encodes two structurally distinct proteins, $p16^{Ink4a}$ and $p19^{ARF}$, both of which restrict cellular proliferation in response to aberrant mitogenic signaling (Jacobs et al., 1999). Bmi-1 has been implicated in the modulation of self-renewal in several types of stem cells, including hematopoietic (Park et al., 2003), neural (Molofsky et al., 2005), and mammary (Liu et al., 2006) . Bmi-1 gene amplification and protein over-expression are also commonly found in cancers of these tissues. In the hematopoietic system, Bmi-1 is required for the proliferation and tumor initiating capacities of leukemic stem cells (Lessard and Sauvageau, 2003). In the nervous system, Bmi-1 is a marker of poor prognosis in oligodendroglial tumors (Hayry et al., 2008), and is essential for the tumorigenicity of neuroblastoma cells (Cui et al., 2007). These observations suggest that inherent self-renewal pathways like Bmi-1 are important for the maintenance of both normal stem cells and cancer cells of a given tissue.

Prostate cancer is the most frequently diagnosed non-skin cancer and second most common cause of cancer related deaths in men (Carson, 2006). Patients not suitable for radiotherapy or surgery are treated with androgen ablation therapy, which effectively shrinks androgen-dependent tumors (Huggins and Hodges, 1941). Unfortunately, this treatment is often followed by recurrent androgen-independent prostate cancer, with frequent metastases (Shaw et al., 2007). The existence of prostate stem cells was elucidated when Isaacs and colleagues found that a fraction of prostate cells remain after castration induced involution, and are capable of regenerating the full gland with all of its different cell lineages (Isaacs, 1987). Certain prostate cancer cells share properties with normal adult prostate stem cells, and have the ability to survive androgen ablation therapy and subsequently regenerate the tumor with a more aggressive phenotype (Litvinov et al., 2003).

Bmi-1 is over-expressed in prostate cancer with adverse pathologic and clinical features. Tumors with Gleason scores of 8 or higher have a significant up-regulation of Bmi-1, while the presence of Bmi-1 in lower grade prostate cancer samples is highly predictive for prostate-specific antigen (PSA) recurrence (van Leenders et al., 2007). Microarray meta-analyses have found that the presence of Bmi-1 in prostate cancer specimens often indicates metastatic disease and a high probability of unfavorable therapeutic outcome (Glinsky et al., 2005). Bmi-1 has been shown enriched in a population of prostate cancer cells with higher tumor initiating capacities (Hurt et al., 2008). These observations allude to the functional involvement of Bmi-1 in prostate cancer progression and maintenance. The ability of Bmi-1 to control stem cell maintenance in other tissues raises the question of whether Bmi-1 is an important regulator of self-renewal in the prostate, and whether this gene is involved in prostate cancer development.

In the present studies, an *in vitro* sphere forming assay and mouse tissue regeneration systems were used to elucidate the role of Bmi-1 in regulating normal mouse prostate stem cell (PrSC) self-renewal and cancer initiation. Lentiviral-delivered shRNAs and over-expression clones were used to show that modulation of Bmi-1 expression levels control prostate stem cell self-renewal activity *in vitro* and prostatic tubule regeneration *in vivo*. P63 is a marker for the more stem-like basal cells of the prostate, which have higher self-renewal capacities. One novel way that Bmi-1 was found to control self-renewal was through the expansion and depletion of these $p63^{+}$cells in spheres, which in turn affected their ability to passage. Transgenic mice were used to show that heightened β-catenin signaling can also increase self-renewal activity in PrSCs. Bmi-1 loss reverses this added self-renewal activity, further highlighting the requirement of Bmi-1 in normal PrSC self-renewal. *In vivo*, loss of

Bmi-1 prevents hyperplastic growth induced by paracrine growth factor signaling in primary prostate cells, and attenuates the growth of prostate cancer induced by a potent cell autonomous oncogene.

RESULTS

Bmi-1 is expressed in the stem cell enriched population of adult prostate

Adult prostate stem cells (PrSCs) are thought to be in the basal compartment since basal cells preferentially survive androgen ablation (English et al., 1987) and can give rise to luminal cells (Robinson et al., 1998). PrSCs are concentrated in the region proximal to the urethra, as BrdU pulse-chase experiments have shown label-retaining cells in that region (Tsujimura et al., 2002). FACS sorting techniques have been used to confirm that cells with stem-like capabilities like self-renewal, multilineage differentiation, and tissue regeneration are highly enriched in the proximal region (Goto et al., 2006; Lawson et al., 2007). Using CD49f and Sca-1 surface markers, we can highly enrich the luminal ($CD49f^{lo}Sca\text{-}1^{-}$) and stem/basal ($CD49f^{hi}Sca\text{-}1^{+}$) cells from adult prostate (Lawson et al., 2010). Q-PCR analysis of these populations reveals a 7 fold higher Bmi-1 mRNA level in the basal/stem cell population than in the more differentiated luminal cells (Figure 1A). Immunohistochemical analyses of adult prostate sections show Bmi-1^{+} cells are enriched in the proximal region of the prostate (Figure 1B). The majority of these cells co-express the basal marker cytokeratin 5 (Figure 1C). Bmi-1 mRNA levels are also significantly higher in prostates from castrated mice, which naturally contain a higher percentage of stem cells (Figure 1D). Higher Bmi-1 expression in the region and cell population enriched for PrSCs indicates that Bmi-1 may play a role in their maintenance.

Bmi-1 regulates self-renewal activity in adult prostate stem cells

Stem cells from the mammary gland and brain have been successfully maintained and passaged *in vitro* as floating spheroids (Dontu et al., 2003; Reynolds and Weiss, 1996). Sphere numbers over multiple passages represents self-renewal activity, while sphere size demonstrates progenitor cell proliferation (Dontu et al., 2004). PrSCs can be maintained in a semi-solid sphere assay, where they give rise to clonally derived spheres and can be passaged for 12 generations, demonstrating self-renewal activity (Xin et al., 2007). An shRNA-assisted knock-down strategy was used to study the functional effect of Bmi-1 loss on adult prostate sphere formation and self-renewal.

We constructed lentiviral vectors that contain a potent shRNA targeting Bmi-1, or a scrambled (Scr) shRNA under the control of the H1 promoter and co-expressing RFP. To rule out off-target effects of shRNA, a rescue Bmi-1 clone (Bmi-1^{Res}) was created by introduction of three silent point mutations into the shRNA target region of murine Bmi-1 (Figure 2A). Knock-down and rescue efficiencies were tested in primary prostate cells and measured by western blot (Figure 2B). Dissociated primary prostate cells were infected with lentivirus containing scrambled or Bmi-1 shRNA, or co-infected with Bmi-1 shRNA and Bmi-1^{Res}, and plated in the prostate sphere assay. After 8 days in culture, there was no difference in the numbers of spheres formed from the mock and scrambled shRNA infected cells. In contrast, the Bmi-1 shRNA infected cells had a 4-fold decrease in sphere forming activity (Figure 2C). Introduction of Bmi-1^{Res} completely rescued the sphere forming activity of the prostate cells, ruling out off target effects. Bmi-1 knock-down spheres were on average 6-fold smaller in diameter than the control spheres, and introduction of Bmi-1^{Res} rescued this phenotype as well (Figures 2D). Bmi-1 is known to epigenetically repress p16 and p19, which could affect proliferation. To elucidate whether these pathways contribute to the decrease in sphere numbers and sizes, scrambled and Bmi-1 shRNA infected spheres were analyzed by Q-PCR and Western. Spheres with lower levels of Bmi-1 showed a 35-

fold increase in the mRNA levels of p16 and p19, which was confirmed at the protein level (Figure S1A and S1B). Lentivirus mediated co-infection of prostate cells with p16 and p19 had a similar inhibitory effect on sphere formation as Bmi-1 shRNA (Figure S2).

Scrambled and Bmi-1 shRNA infected spheres were dissociated and passaged for several generations to test the effect of Bmi-1 inhibition on self-renewal (Figure 2E). While scrambled shRNA infected cells maintain a steady level of sphere forming activity, cells lacking Bmi-1 had a progressive decrease in self-renewal and the capacity to form daughter spheres (Figure 2F). Since only stem-like cells can give rise to new prostate spheres, the diminished sphere formation represents a lower frequency of stem-like cells in the absence of Bmi-1.

A lentiviral delivery system was also used to introduce exogenous Bmi-1 in primary prostate cells to test whether heightened expression would confer added self-renewal. Since Bmi-1 is a known oncogene, we used prostate cells from $p53^{-/-}$ mice in the over-expression studies to minimize oncogenic stress induced apoptosis. We observed no difference in the numbers of primary spheres that formed, indicating that additional Bmi-1 does not confer sphere forming activity to the more differentiated prostate cells. Spheres from both conditions were dissociated and passaged for four generations, and there was a progressive increase in the sphere forming activity of the Bmi-1 infected cells (Figure 2G). Cells with heightened Bmi-1 expression also formed larger spheres than the control infected spheres. Q-PCR and Western analyses of spheres infected with GFP or Bmi-1 revealed a significant decrease in p16 and p19 mRNA and protein levels (Figure S1C and S1D). Therefore, the increase in self-renewal and proliferation in response to heightened Bmi-1 expression is at least partially achieved by a loss of p16 and p19 driven senescence and apoptosis.

Bmi-1 regulates the maintenance of self-renewing cells in the prostate

The LSC and $LSCT^{hi}$ cell populations mark the stem cell fraction in normal prostate (Goldstein et al., 2008; Lawson et al., 2007). Once prostate cells are cultured, Sca-1 gets turned on, the antigenic profile of the sphere cells shift, and quantification of PrSCs becomes less reliable. The LSC and $LSCT^{hi}$ fractions were analyzed in Bmi-1 over-expression and knock-down spheres, and showed trends towards increased and decreased stem cell populations, respectively (Figure S3). An alternative marker for the more primitive prostate cells was also analyzed. p63 has been shown to be crucial for normal prostate development (Signoretti et al., 2000). p63 is almost exclusively expressed in the LSC population (Lawson et al., 2010). $p63^{+}$ cells have significantly higher self-renewal activity than $p63^{-}$ cells (Xin et al., 2007), further indicating that p63 marks the more stem-like cells of the prostate. Sphere sections from Bmi-1 knock-down and over-expression experiments were stained for p63, counterstained with DAPI, and the average percentages of $p63^{+}$ cells were calculated to account for the differences in sphere sizes. There is a 7-fold loss of $p63^{+}$ cells in the Bmi-1 shRNA infected prostate spheres (Figure 3A and 3B). In contrast, sections of $p53^{-/-}$ spheres infected with exogenous Bmi-1 show a 2-fold increase in the number of $p63^{+}$ cells over GFP infected $p53^{-/-}$ spheres (Figures 3C and 3D). Prostate cells infected with Scrambled or Bmi-1 shRNA, and GFP or Bmi-1 lentivirus were analyzed 5 days after infection to test whether p63 was directly regulated by Bmi-1. p63 expression did not change significantly in any of the conditions at the mRNA or protein level (Figure S4). We conclude that the changes in p63 expression patterns are due to altered self-renewal in the $p63^{+}$ population, rather than Bmi-1 modulating the transcription or translation of p63.

Individual RFP^{+} spheres from the scrambled shRNA and Bmi-1 shRNA infected wells were picked, combined with non-colored WT spheres, digested, and passaged to functionally assess changes in stem cell populations. While almost all scrambled shRNA infected spheres produces an average of 25 daughter spheres, only 30 percent of Bmi-1 shRNA infected

spheres were able to passage at all, producing only 1-2 smaller secondary spheres (Figures 3E, 3F and Table S1). Conversely, exogenous Bmi-1 infected prostate spheres formed approximately 35% more daughter spheres than GFP infected spheres, which were also larger in size (Figures 3G, 3H, and Table S1). The shift in the $p63^{+}$ stem-like population and the resulting changes in individual sphere forming capacity corroborate that Bmi-1 expression levels modulate self-renewal activity.

Bmi-1 is necessary for β-catenin induced self-renewal

Many of the self-renewal pathways are interconnected *in vivo*. Studies suggest that Hedgehog (Hh) signaling is important for normal prostate and mammary regeneration and tumor progression (Fiaschi et al., 2009; Karhadkar et al., 2004). Bmi-1 acts down-stream of Hh, and it is the level of Bmi-1 that ultimately controls self-renewal (Liu et al., 2006). This demonstrates the necessity of Bmi-1 expression for Hh induced self-renewal. Wnt signaling has also been shown to be active in PrSCs (Ontiveros et al., 2008), and modulation of β-catenin activity leads to altered sphere forming capacity of prostate cancer cells (Bisson and Prowse, 2009). We investigated the effects of Bmi-1 loss in the presence of over-activated Wnt signaling to elucidate whether Bmi-1 expression is required for other pathways to modulate self-renewal in the prostate.

β-catenin is the key downstream signaling component of the Wnt pathway. Stabilizing mutations in exon 3 of β-catenin (Catnb) over-activate the pathway, and have been reported in many cancers (Morin et al., 1997). The conditional exon 3 knock out mouse ($Catnb^{+/lox(ex3)}$) mimics such mutations, and Wnt signaling is over-activated by introduction of Cre recombinase (Harada et al., 1999). Over-activation of β-catenin during prostate development increases the LSC population ~2.5-fold in the prostate (Data not shown). Dissociated $Catnb^{+/lox(ex3)}$ prostate cells were infected with RFP or Cre lentivirus to over-activate β-catenin signaling, then plated in the sphere assay and passaged (Figure 4A) to determine whether heightened β-catenin signaling affects sphere formation and self-renewal in the prostate. Cre infected $Catnb^{+/lox(ex3)}$ cells had significantly higher sphere forming capacity in generation 1, and increased self-renewal in generation 2 (Figure 4B). Western blot analysis shows that Cre infected spheres have the exon 3 excised form of β-catenin (bottom band) in addition to the WT protein (top band). The mRNA and protein levels of target genes c-Myc and Cyclin D1 increased in the Cre infected spheres, confirming increased β-catenin signaling (Figure 4C and 4D). Bmi-1 mRNA levels were not significantly increased and its predominant target genes p16 and p19 were not affected, indicating little to no change in Bmi-1 signaling with stabilized β-catenin.

$Catnb^{+/lox(ex3)}$ primary prostate cells were infected with Cre/scrambled or Cre/Bmi-1 shRNA lentivirus, to investigate the effects of Bmi-1 loss in the presence of heightened β-catenin signaling. Cre/scrambled shRNA infection increased sphere forming activity and sphere size (Figure 4E). In contrast, Cre/Bmi-1 shRNA infected cells formed significantly fewer and smaller spheres than even the non-infected $Catnb^{+/lox(ex3)}$ cells (Figure 4E). p16 and p19 levels increased upon Bmi-1 inhibition, which must have contributed to this result (Figure S1E). The difference in sphere forming activity was even more striking upon passaging, indicating that loss of Bmi-1 not only reverses the gain of self-renewal activity induced by heightened Wnt signaling, but represses it even further. Introduction of $Bmi\text{-}1^{Res}$ rescued both sphere forming activity and sphere size (Figure S5). These results highlight the importance of Bmi-1 in stem cell maintenance, and suggest that Bmi-1 presence is required for full functional activity of at least one independent self-renewal pathway.

Bmi-1 inhibition decreases tubule forming activity *in vivo*

Another unique property of stem cells is the capacity to regenerate tissue after injury. The *in vivo* prostate regeneration assay can measure this activity (Xin et al., 2003). The PrSC enriched population of prostate cells can regenerate prostatic tubules in SCID mice both subrenally in collagen, and subcutaneously, when injected in Matrigel (Lawson et al., 2007). We tested whether Bmi-1 inhibition alters this PrSC property.

Dissociated prostate cells from C57/Bl6 mice were infected with scrambled or Bmi-1 shRNA lentivirus, and cultured *in vitro* in Matrigel for 72 hours to allow for viral integration and fluorescent protein expression. Infected cells were sorted using FACS, gating on RFP expression. Sorted cells were combined with UGSM and injected subcutaneously into SCID mice (Figure 5A). After 10 weeks, grafts were harvested and analyzed for the presence of fluorescence signal. Bmi-1 shRNA grafts contained little to no red fluorescence signal, while the scrambled shRNA grafts had several red tubules visible under the dissecting microscope (Figure 5B top, and Table S2). Microscopic analysis of H&E sections and fluorescence signal confirms that significantly fewer and smaller tubules were regenerated upon Bmi-1 inhibition (Figure 5B, bottom, and 5C). Both grafts contained a few non-colored tubules, which likely grew from residual non-infected prostate cells. Quantification of the average number of fluorescent tubules per viewing field shows an 85% decrease in tubules (Figure 5C). Since both scrambled and Bmi-1 shRNA infected cells were sorted after infection using the same sorting gate, we can be certain that equal numbers of cells with similar infection levels were implanted. Therefore, the decrease in tubule regeneration activity can only be attributed to the loss of Bmi-1. Bmi-1 shRNA infected tubules express cytokeratin 8 and AR, but have low cytokeratin 5 and p63 expression, indicating a more differentiated state (Figure S6).

Loss of Bmi-1 protects prostate cells from FGF10 driven hyperplasia

Similar to human prostate cancer, Bmi-1 is over-expressed in mouse models of prostate cancer. Heightened Fibroblast Growth Factor (FGF) 10 signaling in UGSM cells leads to a hyperplastic phenotype in nearby mouse epithelium (Memarzadeh et al., 2007). Analysis of such regenerated grafts reveals higher Bmi-1 staining in the hyperplastic epithelium exposed to the FGF 10 expressing UGSM than in the normal tubules grown with control UGSM (Figure S7A). If prostate cancer cells exploit the normal stem cell pathways, then modulating Bmi-1 may attenuate the initiation of cancer.

Primary prostate cells infected with scrambled or Bmi-1 shRNA were combined with FGF10 infected UGSM cells (Figure 6A). After 8 weeks *in vivo*, cells infected with Bmi-1 shRNA formed smaller grafts, as shown by weight and size (Figure 6B and 6C, top panel). Fluorescence images confirm that Bmi-1 shRNA grafts contain fewer and smaller tubules, even in the presence of heightened FGF10 signaling (Figure 6C, bottom panel). Histological analysis reveals that uninfected and scrambled shRNA infected tubules had a mostly hyperplastic phenotype that closely resembles high grade mPIN lesions (Figure 6D), similar to previously reported studies (Memarzadeh et al., 2007). In contrast, the majority of Bmi-1 shRNA infected tubules contained a single or double layer of cells and retained a normal appearance in the presence of heightened FGF10 (Figure 6D). Infected regions from 10 histological sections from 3 representative grafts each were counted and classified as normal or hyperplastic. While ~85% of scrambled shRNA infected tubules had a hyperplastic phenotype, 90% of the Bmi-1 shRNA infected tubules appeared normal (Figure 6E), despite growing in an environment with high FGF10 expression.

Immunofluorescence analysis reveals that uninfected and scrambled shRNA infected regions have increased AR and p63 expression along with increased Ki67 staining. The region

infected with Bmi-1 shRNA contains few p63 positive cells and Ki67 positive cells, again resembling normal tubules in the regeneration assay (Figure 6F). These results show that Bmi-1 expression and the self-renewal and proliferative properties it allows are necessary for prostate epithelial cells to respond to FGF10 signaling induced transformation.

Loss of Bmi-1 attenuates oncogenic progression in the Pten-null prostate cancer model

PTEN (phosphatase and tensin homolog deleted on chromosome 10) is a potent tumor suppressor gene that is frequently mutated in prostate cancer. Cre/Lox mediated conditional deletion of *Pten* in the murine prostate recapitulates the disease progression in humans (Wang et al., 2006). Bmi-1 is up-regulated in the Pten-null prostate at the mRNA and protein levels (Figure S7B and C). Dissociated prostate cells from $Pten^{LoxP/LoxP}$ mice were infected with lentivirus containing either Cre/scrambled, or Cre/Bmi-1 shRNA (Figure 7A). Grafts harvested after 8 weeks reveal that cells infected with Cre/scrambled shRNA formed large tumors (Figure 7B). The $Pten^{LoxP/LoxP}$ cells infected with Cre/Bmi-1 shRNA were also transformed, but the grafts were significantly smaller in size (Figure 7B). The Cre/scrambled shRNA infected grafts had a much more densely packed appearance (Figure 7C), while the Cre/Bmi-1 shRNA infected tumors had lower cellular content (Figure 7D top panels). There were fewer Ki67+ proliferating cells and more TUNEL positive apoptotic cells in the Cre/Bmi-1 shRNA grafts compared to the Cre/scrambled shRNA grafts (Figure 7C and D bottom panels). Altering a single self-renewal gene in the prostate significantly attenuates the initiation and growth of an aggressive form of prostate cancer by affecting proliferation and apoptosis in the cancer cells.

DISCUSSION

Our finding that Bmi-1 loss induces an exhaustion of PrSCs and a depletion of the LSC stem cell fraction as well as the $p63^+$ primitive cells is similar to what is seen in postnatal hematopoiesis, where loss of Bmi-1 significantly reduces the number of HSCs (Park et al., 2003). Bmi-1 is also required for the self-renewal of stem cells in the peripheral and central nervous system, and loss of Bmi-1 results in postnatal growth retardation and neurological defects (Molofsky et al., 2005). These results highlight the conserved role of Bmi-1 across cells derived from all three germ layers.

Bmi-1 has been shown to regulate leukemic stem cell self-renewal as well (Lessard and Sauvageau, 2003). Loss of Bmi-1 in HSCs did not prevent primary leukemia formation. Only when leukemic cells were transplanted into secondary recipients was there a difference in leukemiagenesis. In contrast, loss of Bmi-1 completely prevented the formation of prostate hyperplasia in the FGF10 model, and significantly attenuated the primary outgrowth of prostate cancer induced by Pten deletion.

Bmi-1 expression patterns also vary between tissues. Bmi-1 lineage tracing experiments in pancreas show that $Bmi\text{-}1^+$ cells are differentiated and co-express lineage markers and Ki67, indicating that Bmi-1 is present in more differentiated proliferating cells. The detection of $Bmi\text{-}1^+$ cells one year after pulse-chase marking experiments indicates that Bmi-1 is also present in a subpopulation of self-renewing pancreatic acinar cells (Sangiorgi and Capecchi, 2009). In contrast, Bmi-1 is only expressed in the stem cells of the intestine, and the $Bmi\text{-}1^+$ cells do not co-stain for differentiation markers (Sangiorgi and Capecchi, 2008). Our cell fractionation studies reveal that Bmi-1 expression is highest in the prostate basal/stem cell enriched fraction. This fraction can be further divided into $Trop2^{hi}$ stem- and $Trop2^{lo}$ basal-subpopulations (Goldstein et al., 2008). Bmi-1 was highest in the $Trop2^{hi}$ stem cell fraction, but was still present in the $Trop2^{lo}$ basal cell population as well (data not shown), suggesting that Bmi-1 is not solely expressed by the most primitive cells of the prostate. Weissman and colleagues used a Bmi-1-GFP mouse to show similar results in the hematopoietic system,

where Bmi-1 is highest in the HSCs, but also present in certain progenitors (Hosen et al., 2007). Occasionally, Bmi-1 was found in a few adluminal cells in the proximal region of the prostate. These cells may be related to the recently characterized CARNs cells, which represent rare luminal stem cells that have tumor initiating capacities (Wang et al., 2009).

P63 is a transcription factor belonging to the P53 super-family whose deletion causes a failure to develop stratified epithelia and epithelial appendages in mice, in addition to prostate agenesis (Yang et al., 1999). Signoretti et al. complemented p63−/− blastocysts with p63+/+ galactosidase+ embryonic stem cells and found that luminal cells of the prostate originated only from p63+ donors, which suggests the defects of the *p63*-null stem cells in proliferation and self-maintenance (Signoretti et al., 2000). p63 also marks the more stem-like cells in the prostate (Xin et al., 2007).

In our study, Bmi-1 over-expression led to an expansion of these $p63^+$ cells in $p53^{-/-}$ prostate spheres. Furthermore, we observed a breakdown in cellular organization of the spheres, where the $p63^+$ cells normally confined to the outer rim of spheres expanded in towards the middle (Figure 3C). Such adluminal expansion of $p63^+$ cells has also been observed in several models of murine prostate cancer (Memarzadeh et al., 2007; Wang et al., 2006). The FGF10 model of prostate hyperplasia is an over-growth and excessive branching of the basal/stem cell population of prostate cells, characterized by a concomitant expansion of $p63^+$ cells. The most primitive prostate cells, which are also $p63^+$ are the most susceptible to such transformation (Lawson et al., 2010). Our data suggests that inhibition of Bmi-1 was able to prevent this form of hyperplasia because loss of Bmi-1 caused a depletion of this $p63^+$ LSC population. This finding may have important implications in other epithelial cancers, as many are thought to initiate from stem cells.

The evolutionarily conserved pathways Wnt, Sonic Hh (Shh), Notch and the Polycomb Group gene Bmi-1 are consistently found involved in stem cell self-renewal from Drosophila to humans. Interactions between these pathways have been well documented. Both Wnt and Shh signaling are important for neural tube development, neural stem cell proliferation and self-renewal (Michaelidis and Lie, 2008; Patten and Placzek, 2000; Wechsler-Reya and Scott, 1999). Wnt pathway inhibitors can regulate threshold responses to Shh target genes, demonstrating the existence of mechanisms that integrate graded Shh and Wnt signaling to determine cell fate decisions in the neural tube (Lei et al., 2006). Wnt-1, Hh and Bmi-1 have all been shown in mammary stem cells to influence self-renewal and regenerative capacities (Asselin-Labat et al., 2008). Increase in Hh signaling directly up-regulates Bmi-1 expression, and it is the level of Bmi-1 that controls mammary stem cell self-renewal (Liu et al., 2006). Attempts were made to test the importance of Bmi-1 for Hh driven self-renewal in the prostate. In contrast to mammary stem cells, Hh over-activation through Lentiviral overexpression of Gli-1, and the addition of rShh to PrSCs did not result in a sustained increase in sphere forming and self-renewal activity in our assay (data not shown). Therefore the effects of Bmi-1 inhibition were not tested in these conditions. Interestingly, it also took an extra generation to see significant differences in sphere forming activity in response to Bmi-1 over-expression, while mammary sphere formation increased in generation 1. Both of these findings could be due to the fact that prostate cells are more sensitive to oncogene induced senescence.

β-catenin stabilization did increase self-renewal in the prostate, and Bmi-1 loss reversed this gain of sphere forming activity. In contrast to the interactions between Hh and Bmi-1 in the mammary, β-catenin signaling does not appear to activate Bmi-1 signaling directly and Bmi-1 is likely not downstream of β-catenin. These findings suggest that Bmi-1 and β-catenin are acting in parallel to control self-renewal, and Bmi-1 is necessary for β-catenin to affect this process. Bmi-1 expression and resulting chromosomal modifications may set the

cell to a specific state that allows for self-renewal and proliferation. Even if several developmental pathways are active in certain epithelial stem cells, controlling Bmi-1 may be enough to modulate self-renewal. With the close relationship between stem cell self-renewal and cancer progression, this finding has important implications for controlling cancer growth as well.

EXPERIMENTAL PROCEDURES

Mouse strains

Most animal experiments were conducted using C57BL/6, and $CB17^{Scid/Scid}$ mouse strains, which were originally purchased from The Jackson Laboratory (Bar Harbor, ME). $Pten^{loxP/loxP}$ and $Catnb^{+/Lox(ex3)}$ mice were provided by Dr. Hong Wu. Mice were housed and bred in our animal facilities under the regulation of the Division of Laboratory Animal Medicine at the University of California, Los Angeles.

Prostate Cell Preparation, Cell Sorting, and Primary Cell Culture

The preparation of prostate epithelial cell suspensions from male mice and cell sorting parameters for stem/basal and luminal cell populations were described previously in (Lawson et al., 2010; Lukacs et al., 2010). Prostate sphere assay used for in vitro analysis and passaging has been described by (Xin et al., 2007). Briefly, 5,000 to 50,000 prostate cells were resuspended in 100ul of a 50:50 mixture of Matrigel (BD) and PrEGM (Lonza), and plated around the rim of a well of a 12-well tissue culture plate. Matrigel mix was allowed to solidify at 37°C, and 800ul of PrEGM was added. Media was changed every 3 days. To recover the spheres, wells were treated with 1mg/ml Dispase solution (Gibco). Spheres were digested with Trypsin 0.05% EDTA, triturated through a 27 gauge needle, and filtered through a 40um filter.

Vector Production and Viral Packaging

Third-generation lentiviral vectors FUCGW and FUCRW, derived from FUGW (Lois et al., 2002; Xin et al., 2006), were used for the construction of the Bmi-1 over-expression and all shRNA vectors. Murine Bmi-1 was PCR amplified from a pGEM vector containing the open reading frame of Bmi-1 (a generous gift from Dr. Sean Morrison) and XbaI sites were added for cloning. An shRNA against Bmi-1 was designed to target the mouse *Bmi-1* ORF (TAAAGGATTACTACACGCTAATG). A scrambled shRNA was designed by mutating 3 of the anti-sense nucleotides in the Bmi-1 shRNA sequence. shRNAs were cloned downstream of the H1 promoter. The shRNA resistant clone of murine Bmi-1 was made by introducing 3 silent mutations into the shRNA target region of Bmi-1. Specific cloning steps of all created vectors are provided in Supplemental Data.

Immunohistochemistry

Frozen sections were prepared from 8 week old prostates, and fixed in cold acetone. Prostate spheres and regenerated grafts were fixed in 10% buffered formalin and placed in 70% ethanol. Sections (4μm) were stained with hematoxylin and eosin (H&E) or with specified antibodies. Please see Supplemental Data for specific antibody information. Coverslips were mounted and sections were counterstained with DAPI (Vector), and sections were visualized with fluorescence microscopy.

RNA extraction, q-RT-PCR, and Western Blot Analysis

Sorted cells and dissociated sphere cells were lysed in Buffer RLT and RNA was extracted using RNeasy® Micro Kit (Qiagen). RNA was reverse transcribed using SuperScriptIII®

First Strand kit (Invitrogen). Q-PCR analysis was set up using iQ™ SYBR® Green Supermix kit (BioRad). Primers used for Q-PCR can be found in Supplementary Data.

Dissociated sphere cells were lysed in RIPA buffer (recipe in Supplemental Data). Equal amounts of protein lysates (5-20 μg/lane) were separated by SDS-PAGE (Invitrogen), transferred onto nitrocellulose membranes, which were blocked in 5% milk for 1 hour at RT and blotted with antibody overnight at 4°C (Antibody information in Supplemental Data). Peroxidase-conjugated secondary antibodies (BioRad) were used at 1:10,000 for 1hr at RT. ECL (Millipore) was the chemiluminescent substrate and blots were developed with Kodak Film.

Subcutaneous and Subrenal Prostate Regeneration Assays

The details of the regeneration process have been explained previously (Lukacs et al., 2010). Housing, maintenance, and all surgical procedures were undertaken in compliance with the regulations of the Division of Laboratory Animal Medicine of the University of California, Los Angeles. Briefly, C57Bl6 dissociated prostate cells were infected with scrambled or Bmi-1 shRNA, cultured in Matrigel for 72 hours, and sorted by FACS (for the RFP+ population). Cells were combined with UGSM, mixed with Matrigel, and injected subcutaneously into SCID mice. For the FGF10 experiments, scrambled or Bmi-1 shRNA infected epithelial cells were combined with FGF10 infected UGSM. For the Pten experiments, $Pten^{LoxP/LoxP}$ prostate cells were infected with Cre/Scrambled or Cre/Bmi-1 shRNA lentivirus and combined with wild-type UGSM. Cells were mixed with collagen and implanted under the renal capsule of male SCID mice.

Statistical Analysis

All experiments were performed with at least three different primary cultures or animals in independent experiments. Significance was evaluated by Student's t test. Data are presented as mean +/− SEM.

Supplementary Material

Refer to Web version on PubMed Central for supplementary material.

Acknowledgments

We thank Donghui Cheng, Mireille Riedinger, and Stephanie Wiltzius for assistance with sorting, FGF10 virus preparation, and Cre/shRNA cloning. We thank Andrew Goldstein, David Mulholland, Devon Lawson, Li Xin, Yang Zong and Houjian Cai for helpful discussions about results and the manuscript. Funding sources: ONW is an Investigator of the Howard Hughes Medical Institute and is supported by the Prostate Cancer Foundation Challenge Award for Defining Targets and Biomarkers in Prostate Cancer Stem Cells. RUL is supported by the California Institute for Regenerative Medicine training grant (T1-00005 and TG2-01169). SM is supported by the Ovarian Cancer Research Fund, the Stewart and Lynda Resnik Prostate Cancer Foundation Grant at UCLA, and the Stein/Oppenheimer Clinical Transitional Seed Grant. HW is supported by the Prostate Cancer Foundation, DOD PC031130, NCI UO1 CA84128-06, and RO1 CA107166.

REFERENCES

Asselin-Labat ML, Vaillant F, Shackleton M, Bouras T, Lindeman GJ, Visvader JE. Delineating the epithelial hierarchy in the mouse mammary gland. Cold Spring Harb Symp Quant Biol. 2008; 73:469–478. [PubMed: 19022771]

Bisson I, Prowse DM. WNT signaling regulates self-renewal and differentiation of prostate cancer cells with stem cell characteristics. Cell Res. 2009; 19:683–697. [PubMed: 19365403]

Carson CC 3rd. Carcinoma of the prostate: overview of the most common malignancy in men. N C Med J. 2006; 67:122–127. [PubMed: 16752715]

Cui H, Hu B, Li T, Ma J, Alam G, Gunning WT, Ding HF. Bmi-1 is essential for the tumorigenicity of neuroblastoma cells. The American journal of pathology. 2007; 170:1370–1378. [PubMed: 17392175]

Dontu G, Abdallah WM, Foley JM, Jackson KW, Clarke MF, Kawamura MJ, Wicha MS. In vitro propagation and transcriptional profiling of human mammary stem/progenitor cells. Genes Dev. 2003; 17:1253–1270. [PubMed: 12756227]

Dontu G, Jackson KW, McNicholas E, Kawamura MJ, Abdallah WM, Wicha MS. Role of Notch signaling in cell-fate determination of human mammary stem/progenitor cells. Breast Cancer Res. 2004; 6:R605–615. [PubMed: 15535842]

English HF, Santen RJ, Isaacs JT. Response of glandular versus basal rat ventral prostatic epithelial cells to androgen withdrawal and replacement. Prostate. 1987; 11:229–242. [PubMed: 3684783]

Fiaschi M, Rozell B, Bergstrom A, Toftgard R. Development of mammary tumors by conditional expression of GLI1. Cancer Res. 2009; 69:4810–4817. [PubMed: 19458072]

Gil J, Bernard D, Peters G. Role of polycomb group proteins in stem cell self-renewal and cancer. DNA Cell Biol. 2005; 24:117–125. [PubMed: 15699631]

Glinsky GV, Berezovska O, Glinskii AB. Microarray analysis identifies a death-from-cancer signature predicting therapy failure in patients with multiple types of cancer. The Journal of clinical investigation. 2005; 115:1503–1521. [PubMed: 15931389]

Goldstein AS, Lawson DA, Cheng D, Sun W, Garraway IP, Witte ON. Trop2 identifies a subpopulation of murine and human prostate basal cells with stem cell characteristics. Proceedings of the National Academy of Sciences of the United States of America. 2008; 105:20882–20887. [PubMed: 19088204]

Goto K, Salm SN, Coetzee S, Xiong X, Burger PE, Shapiro E, Lepor H, Moscatelli D, Wilson EL. Proximal prostatic stem cells are programmed to regenerate a proximal-distal ductal axis. Stem cells (Dayton, Ohio). 2006; 24:1859–1868.

Harada N, Tamai Y, Ishikawa T, Sauer B, Takaku K, Oshima M, Taketo MM. Intestinal polyposis in mice with a dominant stable mutation of the beta-catenin gene. EMBO J. 1999; 18:5931–5942. [PubMed: 10545105]

Hayry V, Tynninen O, Haapasalo HK, Wolfer J, Paulus W, Hasselblatt M, Sariola H, Paetau A, Sarna S, Niemela M, et al. Stem cell protein BMI-1 is an independent marker for poor prognosis in oligodendroglial tumours. Neuropathol Appl Neurobiol. 2008; 34:555–563. [PubMed: 18346113]

He S, Nakada D, Morrison SJ. Mechanisms of stem cell self-renewal. Annu Rev Cell Dev Biol. 2009; 25:377–406. [PubMed: 19575646]

Hosen N, Yamane T, Muijtjens M, Pham K, Clarke MF, Weissman IL. Bmi-1-green fluorescent protein-knock-in mice reveal the dynamic regulation of bmi-1 expression in normal and leukemic hematopoietic cells. Stem cells (Dayton, Ohio). 2007; 25:1635–1644.

Huggins C, Hodges C. Studies on prostatic cancer: I. The effects of castration, of estrogen and of androgen injection on serum phosphatases in metastatic carcinoma of the prostate. Cancer Res. 1941; 1:293–297.

Hurt EM, Kawasaki BT, Klarmann GJ, Thomas SB, Farrar WL. CD44+ CD24(−) prostate cells are early cancer progenitor/stem cells that provide a model for patients with poor prognosis. British journal of cancer. 2008; 98:756–765. [PubMed: 18268494]

Isaacs, JT. Control of cell proliferation and cell death in the normal and neoplastic prostate: A stem cell model. Department of Health and Human Services, National Institutes of Health; Bethesda, MD: 1987.

Jacobs JJ, Kieboom K, Marino S, DePinho RA, van Lohuizen M. The oncogene and Polycomb-group gene bmi-1 regulates cell proliferation and senescence through the ink4a locus. Nature. 1999; 397:164–168. [PubMed: 9923679]

Karhadkar SS, Bova GS, Abdallah N, Dhara S, Gardner D, Maitra A, Isaacs JT, Berman DM, Beachy PA. Hedgehog signalling in prostate regeneration, neoplasia and metastasis. Nature. 2004; 431:707–712. [PubMed: 15361885]

Lawson DA, Xin L, Lukacs RU, Cheng D, Witte ON. Isolation and functional characterization of murine prostate stem cells. Proceedings of the National Academy of Sciences of the United States of America. 2007; 104:181–186. [PubMed: 17185413]

Lawson DA, Zong Y, Memarzadeh S, Xin L, Huang J, Witte ON. Basal epithelial stem cells are efficient targets for prostate cancer initiation. Proceedings of the National Academy of Sciences of the United States of America. 2010

Lei Q, Jeong Y, Misra K, Li S, Zelman AK, Epstein DJ, Matise MP. Wnt signaling inhibitors regulate the transcriptional response to morphogenetic Shh-Gli signaling in the neural tube. Dev Cell. 2006; 11:325–337. [PubMed: 16950124]

Lessard J, Sauvageau G. Bmi-1 determines the proliferative capacity of normal and leukaemic stem cells. Nature. 2003; 423:255–260. [PubMed: 12714970]

Litvinov IV, De Marzo AM, Isaacs JT. Is the Achilles' heel for prostate cancer therapy a gain of function in androgen receptor signaling? J Clin Endocrinol Metab. 2003; 88:2972–2982. [PubMed: 12843129]

Liu S, Dontu G, Mantle ID, Patel S, Ahn NS, Jackson KW, Suri P, Wicha MS. Hedgehog signaling and Bmi-1 regulate self-renewal of normal and malignant human mammary stem cells. Cancer Res. 2006; 66:6063–6071. [PubMed: 16778178]

Lois C, Hong EJ, Pease S, Brown EJ, Baltimore D. Germline transmission and tissue-specific expression of transgenes delivered by lentiviral vectors. Science (New York, NY. 2002; 295:868–872.

Lukacs RU, Goldstein AS, Lawson DA, Cheng D, Witte ON. Isolation, cultivation and characterization of adult murine prostate stem cells. Nat Protoc. 2010; 5:702–713. [PubMed: 20360765]

Memarzadeh S, Xin L, Mulholland DJ, Mansukhani A, Wu H, Teitell MA, Witte ON. Enhanced paracrine FGF10 expression promotes formation of multifocal prostate adenocarcinoma and an increase in epithelial androgen receptor. Cancer cell. 2007; 12:572–585. [PubMed: 18068633]

Michaelidis TM, Lie DC. Wnt signaling and neural stem cells: caught in the Wnt web. Cell Tissue Res. 2008; 331:193–210. [PubMed: 17828608]

Molofsky AV, He S, Bydon M, Morrison SJ, Pardal R. Bmi-1 promotes neural stem cell self-renewal and neural development but not mouse growth and survival by repressing the p16Ink4a and p19Arf senescence pathways. Genes Dev. 2005; 19:1432–1437. [PubMed: 15964994]

Morin PJ, Sparks AB, Korinek V, Barker N, Clevers H, Vogelstein B, Kinzler KW. Activation of beta-catenin-Tcf signaling in colon cancer by mutations in beta-catenin or APC. Science (New York, NY. 1997; 275:1787–1790.

Ontiveros CS, Salm SN, Wilson EL. Axin2 expression identifies progenitor cells in the murine prostate. Prostate. 2008; 68:1263–1272. [PubMed: 18563716]

Pardal R, Molofsky AV, He S, Morrison SJ. Stem cell self-renewal and cancer cell proliferation are regulated by common networks that balance the activation of proto-oncogenes and tumor suppressors. Cold Spring Harb Symp Quant Biol. 2005; 70:177–185. [PubMed: 16869752]

Park IK, Qian D, Kiel M, Becker MW, Pihalja M, Weissman IL, Morrison SJ, Clarke MF. Bmi-1 is required for maintenance of adult self-renewing haematopoietic stem cells. Nature. 2003; 423:302–305. [PubMed: 12714971]

Patten I, Placzek M. The role of Sonic hedgehog in neural tube patterning. Cell Mol Life Sci. 2000; 57:1695–1708. [PubMed: 11130176]

Reya T, Morrison SJ, Clarke MF, Weissman IL. Stem cells, cancer, and cancer stem cells. Nature. 2001; 414:105–111. [PubMed: 11689955]

Reynolds BA, Weiss S. Clonal and population analyses demonstrate that an EGF-responsive mammalian embryonic CNS precursor is a stem cell. Developmental biology. 1996; 175:1–13. [PubMed: 8608856]

Robinson EJ, Neal DE, Collins AT. Basal cells are progenitors of luminal cells in primary cultures of differentiating human prostatic epithelium. Prostate. 1998; 37:149–160. [PubMed: 9792132]

Sangiorgi E, Capecchi MR. Bmi1 is expressed in vivo in intestinal stem cells. Nat Genet. 2008; 40:915–920. [PubMed: 18536716]

Sangiorgi E, Capecchi MR. Bmi1 lineage tracing identifies a self-renewing pancreatic acinar cell subpopulation capable of maintaining pancreatic organ homeostasis. Proceedings of the National Academy of Sciences of the United States of America. 2009; 106:7101–7106. [PubMed: 19372370]

Shaw GL, Wilson P, Cuzick J, Prowse DM, Goldenberg SL, Spry NA, Oliver T. International study into the use of intermittent hormone therapy in the treatment of carcinoma of the prostate: a meta-analysis of 1446 patients. BJU Int. 2007; 99:1056–1065. [PubMed: 17346277]

Signoretti S, Waltregny D, Dilks J, Isaac B, Lin D, Garraway L, Yang A, Montironi R, McKeon F, Loda M. p63 is a prostate basal cell marker and is required for prostate development. The American journal of pathology. 2000; 157:1769–1775. [PubMed: 11106548]

Tsujimura A, Koikawa Y, Salm S, Takao T, Coetzee S, Moscatelli D, Shapiro E, Lepor H, Sun TT, Wilson EL. Proximal location of mouse prostate epithelial stem cells: a model of prostatic homeostasis. The Journal of cell biology. 2002; 157:1257–1265. [PubMed: 12082083]

van Leenders GJ, Dukers D, Hessels D, van den Kieboom SW, Hulsbergen CA, Witjes JA, Otte AP, Meijer CJ, Raaphorst FM. Polycomb-group oncogenes EZH2, BMI1, and RING1 are overexpressed in prostate cancer with adverse pathologic and clinical features. European urology. 2007; 52:455–463. [PubMed: 17134822]

van Lohuizen M, Verbeek S, Scheijen B, Wientjens E, van der Gulden H, Berns A. Identification of cooperating oncogenes in E mu-myc transgenic mice by provirus tagging. Cell. 1991; 65:737–752. [PubMed: 1904008]

Wang S, Garcia AJ, Wu M, Lawson DA, Witte ON, Wu H. Pten deletion leads to the expansion of a prostatic stem/progenitor cell subpopulation and tumor initiation. Proceedings of the National Academy of Sciences of the United States of America. 2006; 103:1480–1485. [PubMed: 16432235]

Wang X, Kruithof-de Julio M, Economides KD, Walker D, Yu H, Halili MV, Hu YP, Price SM, Abate-Shen C, Shen MM. A luminal epithelial stem cell that is a cell of origin for prostate cancer. Nature. 2009; 461:495–500. [PubMed: 19741607]

Wechsler-Reya RJ, Scott MP. Control of neuronal precursor proliferation in the cerebellum by Sonic Hedgehog. Neuron. 1999; 22:103–114. [PubMed: 10027293]

Xin L, Ide H, Kim Y, Dubey P, Witte ON. In vivo regeneration of murine prostate from dissociated cell populations of postnatal epithelia and urogenital sinus mesenchyme. Proceedings of the National Academy of Sciences of the United States of America. 2003; 100(Suppl 1):11896–11903. [PubMed: 12909713]

Xin L, Lukacs RU, Lawson DA, Cheng D, Witte ON. Self-renewal and multilineage differentiation in vitro from murine prostate stem cells. Stem cells (Dayton, Ohio). 2007; 25:2760–2769.

Xin L, Teitell MA, Lawson DA, Kwon A, Mellinghoff IK, Witte ON. Progression of prostate cancer by synergy of AKT with genotropic and nongenotropic actions of the androgen receptor. Proceedings of the National Academy of Sciences of the United States of America. 2006; 103:7789–7794. [PubMed: 16682621]

Yang A, Schweitzer R, Sun D, Kaghad M, Walker N, Bronson RT, Tabin C, Sharpe A, Caput D, Crum C, et al. p63 is essential for regenerative proliferation in limb, craniofacial and epithelial development. Nature. 1999; 398:714–718. [PubMed: 10227294]

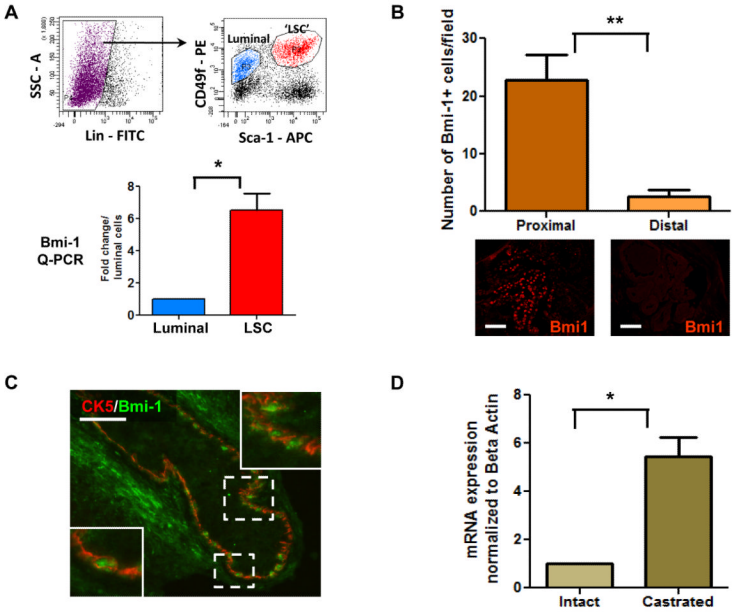

Figure 1. Bmi-1 is expressed in prostate stem cell enriched regions and cell fractions

(A) FACS plots of the luminal ($CD49f^{lo}Sca\text{-}1^{-}$, blue) and 'LSC' basal/stem ($CD49f^{+}Sca\text{-}1^{+}$, red) cell populations. Graph shows Bmi-1 mRNA levels in the luminal and LSC cells of adult mouse prostate. (B) Quantification of the Bmi-1^{+} cells in the proximal and distal regions of adult prostate. Representative images show Bmi-1 staining in these regions. Bar=100μm. (C) Image shows representative area from the proximal region co-stained with Bmi-1 and cytokeratin (CK) 5. Scale bar=50μm (D) Bmi-1 mRNA levels in intact and castrated 8 week old prostates. Data shown as mean +/− SEM

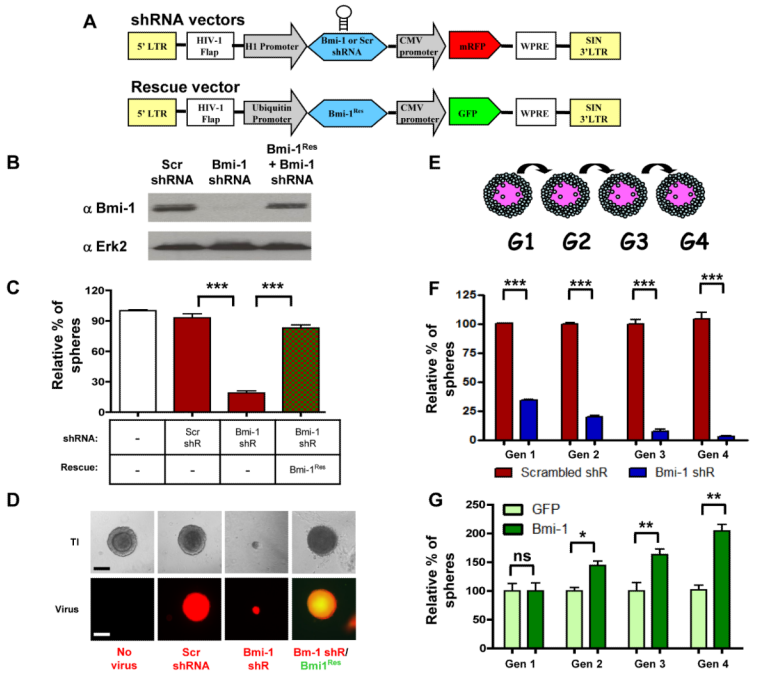

Figure 2. Bmi-1 expression controls sphere-formation and self-renewal in adult prostate stem cells

(A) Diagram of shRNA and Bmi-1Res lentivector constructs. (B) Western blot of scrambled (Scr) shRNA, Bmi-1 shRNA, and Bmi-1 shRNA/Bmi-1Res infected prostate cell lysates. (C) Frequency of primary prostate spheres formed from infected cells. Sphere counts are normalized to mock-infected spheres. (D) Representative sphere images from each condition – transilluminating (TI), and fluorescence images show viral infection with respective shRNA (red), and Bmi-1Res (green) virus. Bar=100μm. (E) Schematic of sphere passaging. (F) Scrambled and Bmi-1 shRNA infected prostate spheres were dissociated and equal numbers of cells were passaged for 4 generations. Spheres counts are normalized to the first generation scrambled shRNA spheres. See also Figure S1A, B and S2. (G) Frequency of spheres from GFP and Bmi-1-GFP infected P53−/− prostate cells. Spheres were dissociated and passaged at equal cell numbers for 4 generations. Sphere counts are normalized to generation 1 GFP infected spheres. Data represented as mean +/− SEM. See also Figure S1C and D.

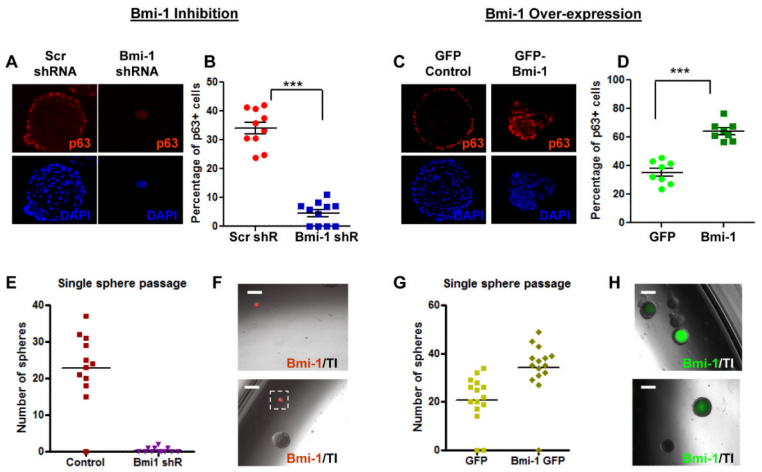

Figure 3. Bmi-1 regulates the depletion and expansion of self-renewing cells in prostate spheres

(A) p63 and DAPI stains of scrambled (left) and Bmi-1 shRNA (right) infected spheres. (B) Percentage of $p63^{+}$ cells in 12 representative scrambled and Bmi-1 shRNA infected spheres. (C) p63 and DAPI stains of GFP (left column) and Bmi-1 (right column) infected $p53^{-/-}$ prostate spheres. (D) Percentage of $p63^{+}$ cells in 12 representative GFP and Bmi-1 infected spheres. (E) Number of daughter spheres formed from single dissociated scrambled and Bmi-1 shRNA infected and (G) GFP and Bmi-1 infected spheres. (F) Merged images of representative daughter spheres formed from Bmi-1 shRNA (red) infected and (H) Bmi-1-GFP (green) infected spheres. Data represented as mean +/− SEM. Bar=200μm. See also Figures S3, S4, and Table S1.

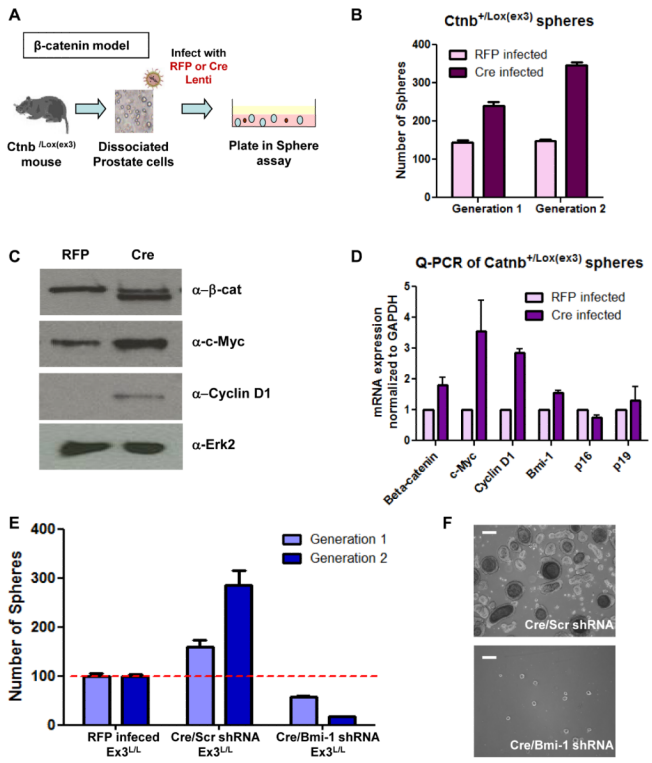

Figure 4. Bmi-1 is required for β-catenin mediated self-renewal

(A) Diagram of experimental approach. (B). Number of spheres formed in two generations of RFP and Cre infected Catnb$^{+/Lox(Ex\ 3)}$ prostate cells. (C) Western blot and (D) Q-PCR analysis of β-catenin, β-catenin target genes, and Bmi-1 expression levels in RFP infected (WT) and Cre infected (Ex3 KO) cells. (E) Frequency of 1° and 2° spheres from RFP, Cre/scrambled, and Cre/Bmi-1 shRNA infected Catnb$^{+/Lox(Ex\ 3)}$ cells normalized to generation 1 RFP spheres. Data represented as mean +/− SEM. (F) Images of representative Cre/scrambled and Cre/Bmi-1 shRNA infected spheres. Bar=200μm. See also Figures S1 and S5.

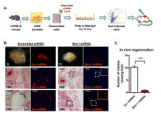

Figure 5. Loss of Bmi-1 decreases *in vivo* prostate tubule formation

(A) Schematic of experimental approach. (B) (Top) TI images of regenerated grafts and fluorescent images of RFP signal that represents infection. (Bottom) H&E and fluorescent images of representative grafts of scrambled and Bmi-1 shRNA infected primary prostate cells. RFP shows integrated virus. Bars=200μm. (C) Average number of RFP^+ tubules per viewing field, calculated from 3 viewing fields from 12 different tissue sections of scrambled and Bmi-1 shRNA infected grafts (9 grafts/condition from 3 experiments were analyzed), represented as mean +/− SEM. See also Figure S6 and Table S2.

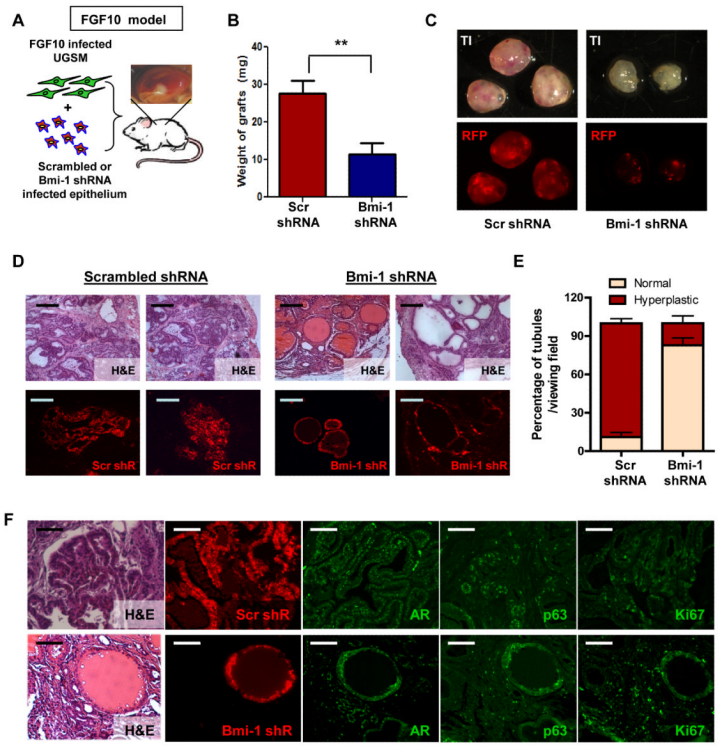

Figure 6. Bmi-1 inhibition protects primary prostate cells from hyperplasia driven by FGF10 signaling

(A) Schematic shows experimental approach. (B) Average weight of 6 scrambled shRNA/FGF10 UGSM and Bmi-1 shRNA/FGF10 UGSM grafts each from 2 experiments. (C) TI (top) and RFP fluorescence images (bottom) of scrambled shRNA/FGF10 (left) and Bmi-1 shRNA/FGF10 (right) grafts. (D) H&E sections show representative tubules from Bmi-1 and scrambled shRNA infected grafts (top). Fluorescence images show representative tubules and their infection status (red) from Bmi-1 and scramble shRNA infected tubules. Bars=200μm. (E) Average percentage of hyperplastic and normal appearing RFP^+ tubules calculated from 10 representative sections from 3 grafts of each condition, represented as mean +/− SEM. (F) H&E and fluorescence images show viral infection status (red), AR (green), p63 (green), and Ki67 (green) staining of a Scrambled shRNA infected region(red) (top) and a Bmi-1 shRNA infected tubule (red) surrounded by non-infected epithelium (non-colored) (bottom). Bars=100μm. See also Figure S7A.

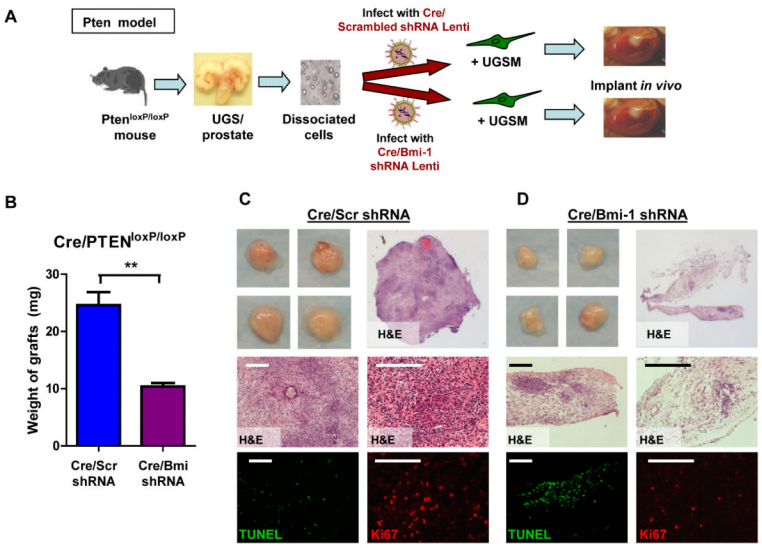

Figure 7. Bmi-1 inhibition attenuates tumor growth from Pten-*null* prostate cells

(A) Schematic of experimental approach. (B) Average weight of Cre/scrambled and Cre/Bmi-1 shRNA infected grafts from 6 grafts each and 2 experiments, represented as mean +/− SEM. (C and D) Representative images and H&E sections (top) show the grafts and microscopic phenotypes of regenerated Cre/scrambled (C) and Cre/Bmi-1 shRNA (D) infected tumors. Fluorescent images (bottom) show Ki67 (red) and TUNEL (green) staining of representative sections. Bars=200μm. See also Figure S7B and C.